IOSR Journal of Computer Engineering (IOSR-JCE)
e-ISSN: 2278-0661,p-ISSN: 2278-8727, Volume 19, Issue 5, Ver. V (Sep.- Oct. 2017), PP 23-34
www.iosrjournals.org

Parallel Random Motion-Selective Rank Band Based Image Compression Using Hybrid Multi Wavelet Transform

B. Sridhar[1], S.Jagadeesh[2]
[1]*SSJ Engineering College,*
[2]*Professor & Head of the Department, SSJ Engineering College, Hyderabad.*
Corresponding Author: B. Sridhar

Abstract: *A Hybrid Multi Wavelet Transform (HMWT) based 2D magnetic resonance (MR) image compression method is proposed. The proposed work presents a novel MR image compression method using Parallel Random Band Selection Method and Motion-Selective Rank Algorithm (PRMRB). In the proposed method, 2D multispectral MR image is spectral decorrelated and temporal decorrelated in the first and second stage of intra and inter band correlation. From this process, the main spectral band component for analysis is selected. These components were given to Parallel Random Band Selection Method, where the registration of sequence of band components is done. In this approach, the spectral bands are treated independently, so there will be many sequences as the number of spectral bands. Motion-Selective Rank Algorithm will generate a multi spectral adaptive sub band wavelet transform filters known multi-directional filters , performs better in terms of motion estimation and compression efficiency, divided in to multi frames of temporal filtering generating HMWT. Throughout the experiments, the proposed novel HMWT shows good performance with the conventional methods.*

Keywords: *Wavelet Transform, magnetic resonance, spectral, band correlation, motion estimation.*

Date of Submission: 23-10-2017 Date of acceptance: 02-11-2017

I. Introduction

Accurate reconstruction of image is important in many image processing applications such as image compression [18] [16] [9] , image denoising [8], image fusion [1] [8], image demosaicking [12] and so on. In image coding [6], the estimation of compression rate, error variance and visual qualities [14] are proven to be very useful parameters for the prediction of quality [3] of image processing technique. 2D MR image compression need more attention compare to the traditional, it is an active topic in the area of Medical Image Analysis (MIA), the compressed MR image should look like a natural original image, and therefore the modeling of such is a crucial to the success of MR image compression.

Recent research focussing on MR image compression [2] [4] [5] [7] has greatly increased the potential of Medical Vision Algorithm (MVA) that keeps patient information and diagnosis results together. These MR image Digital Imaging and Communications in Medicine (DICOM) in .dcm format facilitates a dataset of patient diagnosis report, from the scan display environment to techniques for data collection, to algorithms for area of diagnosis and techniques for displaying, storing and transmitting on a surface.

During the process of storage and transmission, the patient diagnosis report is processed under MVA's to design a lossless and noise free transmission channel with less storage capability with high compression rates. Techniques to perform these actions could not be able to reach all the parameters together.

The issue of 2D MR image compression and transmission is addressed. Proposed method is formulated in the traditional compression algorithm focused on denoising, fusion and demosaicking algorithms. Traditional approaches operate on wavelet decomposing and try to reconstruct the original by approximation. Proposed is - the original image is known, prior to wavelet decomposition band selection is performed, the selected band is processed for motion estimation functions over the image. A discrete multiwavelet is performed on selected coefficients, developed a method that improves the image reconstruction process. Proposed method results demonstrate that proposed method can improve the similarity of compression.

Research in Medical Image Compression recently is developing in the saliency [10], sparse [11] and wavelet transformation techniques [12] [13] [15] [17], to provide improvement in image quality at high compression rates and low bit rates. Wavelet based compression techniques need symmetry and orthogonality to outperform a high degree of processing applications. To perform this, multiwavelet techniques are evolved since, the multiple band decomposition of this process overhead the computation time and band selection. Design of filters for the multiwavelet technique is complex and is possible to make simplex by improving the adaptability and bi-orthogonality. Coefficients of multiwavelet technique are large number and is reduced by

quantizing the number of bits required to represent the wavelet coefficients. With the less number of coefficients the reconstruction quality is to be improved with different bit rates. With the above observations, in this work a 2D MR image compression method is proposed. From the given MR image, estimation of motion vectors of MR image is made. Take this estimated motion, as a reference, select the band of MR image and implement the selected band with PRMRB, ie., motion band selected of the compressed image should be close to the original MR image. As shown in results, the proposed PRMRB method can well enhance the image visual texture regions, which are often could not by other comparative methods.

The remainder of the proposed work is as follows. Section 2 overviews proposed overall methodology for computing the compression method; section 3 shows the results; section 4 and section 5 conclude with a discussion and future work of proposed work.

II. Proposed Work

Implementation of proposed work, begins with the implementation of motion-selective rank and parallel random band selection method. Considering a magnetic resonance (MR) image with spatial-band position of the associated band in MR image.

A. Motion-selective ranking

With the multiwavelet uniform band selection from available bands of the MR image, MR band selection model is of the form

$$f_{\upsilon}(x,y)=\frac{1}{2\pi(\upsilon_x+\upsilon_y)}e^{-\frac{x^2+y^2}{2(\upsilon_x+\upsilon_y)}} \quad (1)$$

The motion MR image is generated by varying the spatial-band positions from different band locations, the model of motion MR image is of the form

$$i_M(x,y)=\sum_m \sum_n f_M(x,y)i(m:x,n:y) \quad (2)$$

where $i\ (x,y)$ and $i_M(x,y)$ are the original and motion MR images respectively and m and n are band ranks. The motion MR sequences are to be appeared similar to original image, to achieve this the validation of (2) is given by

$$i_M(x,y)=conv\left(\sum i\circ f\right]f_M^{-1}(\bullet) \quad (3)$$

where f_M and f_M^{-1} are the proposed forward and inverse wavelet filters, such that

$$i_{Mr}(x,y)=conv\left(\sum i\circ f_M^{-1}\right]f\ \ (\bullet) \quad (4)$$

$$i_{Mf}(x,y)=\left(\sum_m f_M(x,y)i(x,y)\sum_n f_M^{-1}(x,y)i(m:x,n:y)\right] \quad (5)$$

$$i_{Me}(x,y)=conv\left(\sum i\circ i_{Mf}(x,y)\right] \quad (6)$$

shows the wavelet based MR motion image $i_{Mr}(x,y)$ is similar to original image in motion estimation $i_{Me}(x,y)$. Thus, the motion estimated image $i_{Me}(x,y)$ after varying the motion band selection region $i_{Mr}(x,y)$ is a valid uniform band selection wavelet of the original image $i\ (x,y)$ based on motion-selective rank bands.

Considering (2), (4) and (6), it is proved that the filtered MR motion image can be obtained by applying the f_M & f_M^{-1} to the original image and $f_M^{-1}(x,y)i(m:x,n:y)$ rank bands, such that $f_M^{-1}[i(x,y)]$ is the real approximation of varying $f_M^{-1}[i_{Mr}(x,y)]$.

Assuming the proposed f_M & f_M^{-1} wavelet transform filter, can be estimated from the test image (eg. Paris.lan), the proposed wavelet filter allows the motion estimation of original image that are projected in the MR band surface, are shown in figure 1.

a) Original magnetic resonance (MR) 3d_MIP_mra_006.png dataset

b) Gray of a)

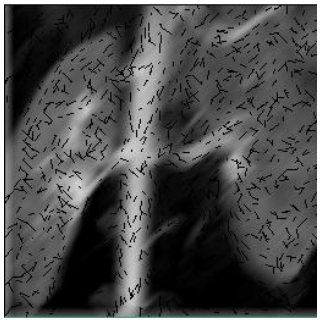

c) Motion Vectors of a)

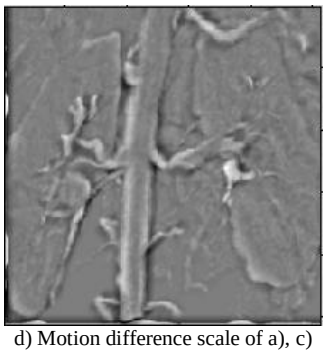

d) Motion difference scale of a), c)

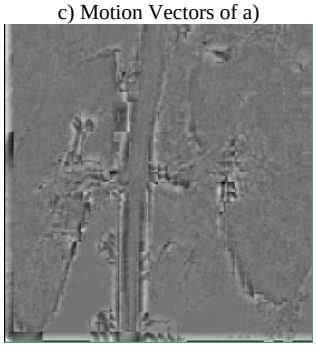

e) Motion Estimations of b), d)

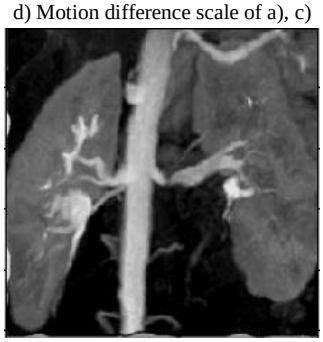

f) Motion Selective Rank band of b), d)

Figure 1 : Observations of proposed motion selective wavelet.

B. Parallel random band selection

Given the motion selective rank band, $i_{Me(\upsilon_x+\upsilon_y)}(x,y)$ compute a set of $i_{Mr}(x,y)$ MR bands with increasing band levels $i_{Ml}(x,y)$, such that

$$i_{Me(\upsilon_x+\upsilon_y)}(x,y) = \sum i_{Me}(x,y)\, f_{M(\upsilon_x+\upsilon_y)}(x,y) \quad (7)$$

where $f_{M(\upsilon_x+\upsilon_y)}(x,y)$ represents the uniform band selection in (1) with band levels $(\upsilon_x+\upsilon_y)$. Typical values of $(\upsilon_x+\upsilon_y)$ =10, 20, 30,..of multiplicative $i_{Ml}(x,y)$ levels. These levels $i_{Ml(\upsilon_x+\upsilon_y)}(x,y)$ serve as random MR band selection for estimating the motive rank bands across the MR image. Parallel correlation can be applied to each level of $(\upsilon_x+\upsilon_y)$ through $i_{Ml}(x,y)$ to find most similar $i_{Ml(\upsilon_x+\upsilon_y)}(x,y)$ for each MR band selection.

The final result is a MR band selection, that assigns the appropriate $(\upsilon_x+\upsilon_y)$ to each $i_{Me(\upsilon_x+\upsilon_y)}(x,y)$ based on $i_{Mr}(x,y)$. Here, use $(\upsilon_x+\upsilon_y)$ to represent the parallel MR band level $f_{Ml(\upsilon_x+\upsilon_y)}(x,y)$ selection, which best approximates the $i_{Me(\upsilon_x+\upsilon_y)}(x,y)$ in MR band region. The selection of each MR band appears as similar to the $i_{Mr(\upsilon_x+\upsilon_y)}(x,y)$, are shown in figure 2.

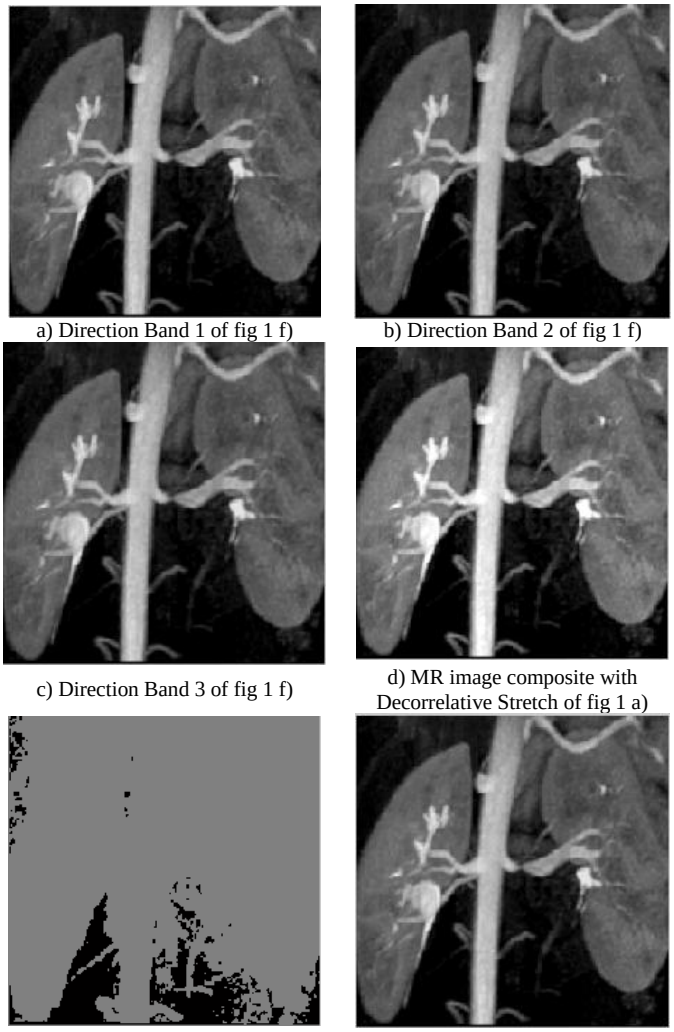

a) Direction Band 1 of fig 1 f) b) Direction Band 2 of fig 1 f)

c) Direction Band 3 of fig 1 f) d) MR image composite with Decorrelative Stretch of fig 1 a)

e) Normalized Difference Vegetation Index of fig 1 f) f) Band Selected Image of d) with a), b), c)

Figure 2 : Observations of proposed parallel random band selection

C. Hybrid Discrete Multiwavelet Transform

Given the band selected image $i_{Ml(\upsilon_x+\upsilon_y)}(x,y)$, an approximate spectral varying wavelet coefficients $i_{map(\upsilon_x+\upsilon_y)}(x,y)$ are selected to map the distinct MR image bands are defined as $i_{d(\upsilon_x+\upsilon_y)}(x,y)$. Using these $i_{d(\upsilon_x+\upsilon_y)}(x,y)$, computation of multidirectional filter images, $i_{multi-d(\upsilon_x+\upsilon_y)}(x,y)$, using MR filters as described in (3), the $i_{multi-d(\upsilon_x+\upsilon_y)}(x,y)$ is updated for each MR band image. The method for compressive coding is made possible by updating the multidirectional filter images:

$$i_{multi-d(\upsilon_x+\upsilon_y)}(x,y) = i_{Ml(\upsilon_x+\upsilon_y)}(x,y) + \delta\left(i_{Me(\upsilon_x+\upsilon_y)}(x,y)\right) \quad (8)$$

where δ is a pre-selected MR band. The coding coefficients $C_q(x,y)$ of each multidirectional filter image are updated by :

$$C_q(x,y) = \psi_q(i, i_{multi-d})\Phi_i i\ (x,y) \quad (9)$$

where $\psi_q(i, i_{multi-d})$ is MR motion learned dictionary and $\Phi_i i\ (x,y)$ is MR reconstruction variable.

By using (8), further updating the (9) continues by coding vector V_i,

$$\mathrm{V}_i = \sum_q \omega_q^{i(x,y)} C_q^{i(x,y)} \circ \mathrm{M}_q^{i(x,y)} \quad (10)$$

where $\omega_q^{i(x,y)}$ is multiwavelet coefficients, $C_q^{i(x,y)}$ is (9) and $\mathrm{M}_q^{i(x,y)}$ is repetitive vector of (8), figure 3 shows the images of these basis and figure 4 shows the filter signals.

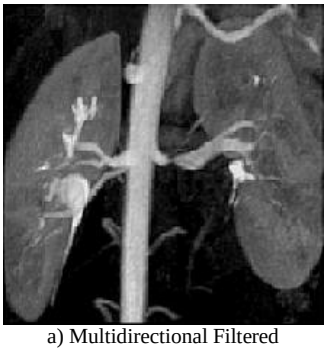

a) Multidirectional Filtered Image of fig 2 f)

b) Filtered Wavelet Image for Compression Coding of a)

Figure 3 : Observations of proposed compression coding process

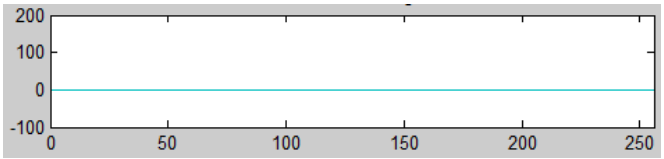

a) Band Selected Signal of fig 2 f)

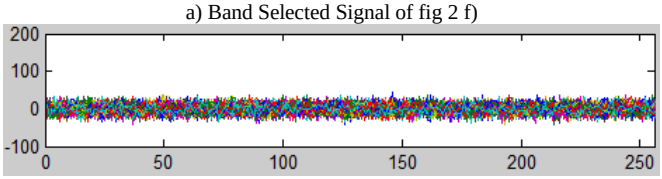

b) Multidirectional Filtered Signal of fig 3 a)

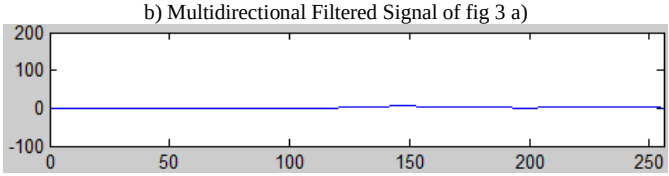

c) Filtered Signal of fig 3 b)

Figure 4 : Observations of proposed filter analysis

In the proposed MR band selection, multiwavelet discrete wavelet transform (DWT) pair is introduced, which is designed to simultaneously process the properties of the multi-level DWT and band-position DWT. Both DWT can outperform in a single wavelet transform MWDWT, that has the process of both the multi-level DWT and band-position DWT. The proposed MWDWT is based on the single wavelet function and two distinct DWT, represented as:

$$\omega_{g,1}(t) = W\left[\omega_{h,1}(t), \omega_{h,2}(t - t_W)\right] \text{ and}$$
$$\omega_{g,2}(t) = W\left[\omega_{h,1}(t - t_W), \omega_{h,2}(t)\right] \quad (11)$$

where W is proposed MWDWT transform pair, $\omega_{h,i}(t)$ and $\omega_{g,i}(t)$ are two distinct DWT and $i = 1,2$ is one single wavelet function, figure 5 shows the images of these basis.

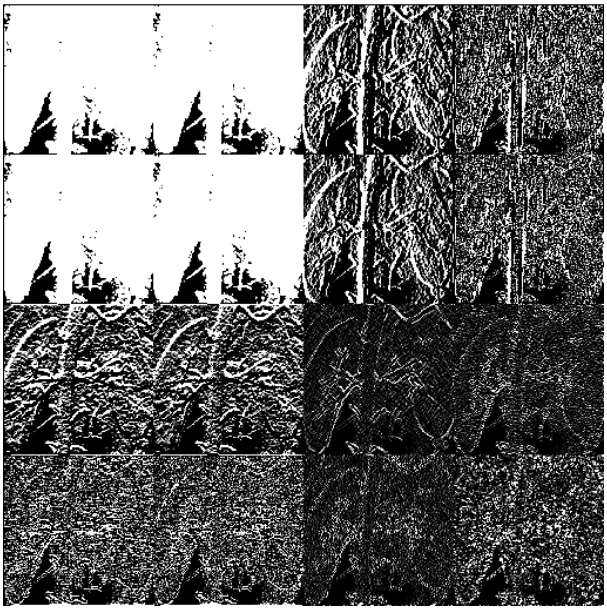

a) Multiwavelet Bands decomposition of fig 3 a)

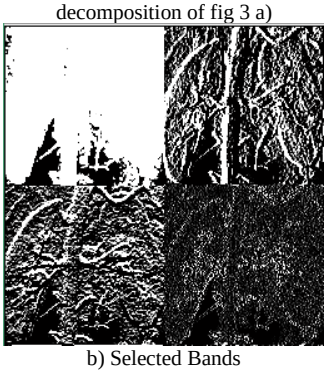

b) Selected Bands decomposition of fig 3 b)

Figure 5 : Observations of proposed MWDWT transform decomposition

From the multiband identities, the perfect reconstruction conditions can be written as:

$$\sum_{i=1}^{2} W^{-1}\left[\omega_{h,1}(t),\omega_{h,2}(t)\right]=\sum_{i=1}^{2} W^{-1}\left[\omega_{h,1}(t-t_W),\omega_{h,2}(t-t_W)\right]=1$$

and

$$\sum_{i=1}^{2} W^{-1}\left[\omega_{h,1}(t-t_W),\omega_{h,2}(t)\right]=\sum_{i=1}^{2} W^{-1}\left[\omega_{h,1}(t),\omega_{h,2}(t-t_W)\right]=2$$

(12)

The reconstructed image figure 1 (a) , is shown in figure 6.

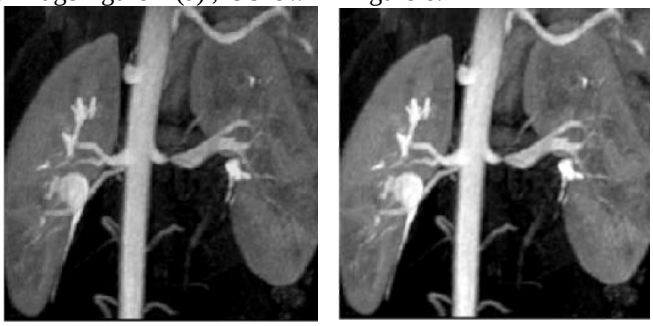

a) Original magnetic resonance (MR) 3d_MIP_mra_006.png dataset

b) Proposed method PRMRB reconstructed image with 88.10 dB PSNR

Figure 6 : Observations of proposed image compression method

III. Results and Discussions

In the proposed work chapter, observations of an MR image compression and reconstruction of PRMRB were shown. In this chapter, application of proposed method on four types of image formats: Multispectral (MS) Paris.Lan format, Mat WDC.Mat format, GIF Gun.gif format and BMP Lena.bmp format. Comparison of proposed method PRMRB is performed on image compression methods Embedded Zerotree Wavelet [18], A New Fast And Efficient Image Codec Based On Set Partitioning In Hierarchical Trees [16] and Binary Tree Coding With Adaptive Scanning Order [9], image fusion methods Robust Multi-Exposure Image Fusion : A Structural Patch Decomposition Approach [1] and Multifocus & Multispectral Image Fusion Based On Pixel Significance Using Discrete Cosine Harmonic Wavelet Transform [8] and image demosaicking method Binary Tree-Based Generic Demosaicking Algorithm For Multispectral Filter Arrays [12].

A. Image Visual Comparative Results

The approach of considering these image processing methods and image formats is to make the readers, the proposed method is applicable to all types of image processing methods and formats. The image representation of four types of image formats are shown in figure 1.

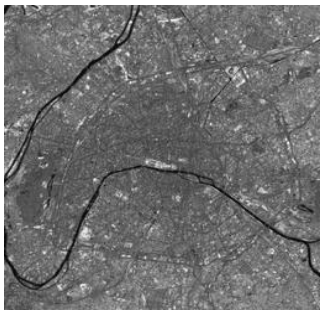

a) Multi Spectral paris.lan

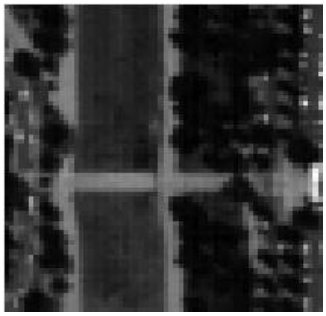

b) WDC.Mat

c) Gun.gif File

d) Lena.bmp

Figure 1: Input Images considered for analysis of proposed method

Multi Spectral paris.lan and Lena.bmp images are compared with [1],[2] and [3], the image visual results are shown in figure 2 and figure 3.

a) [18] reconstructed image with PSNR 26.22 dB

b) [16] reconstructed image with PSNR 36.09 dB

c) [9] reconstructed
image with PSNR 38.36 dB

d) Proposed PRMRB
reconstructed image
with PSNR 57.10 dB

Figure 2 : Comparative Lena.bmp Reconstruction
of proposed PRMRB with [18], [16] and [9].

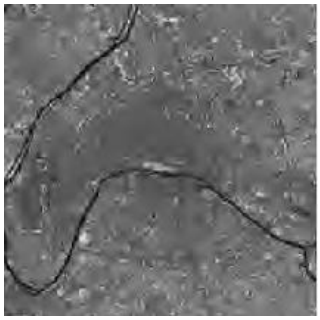

a) [18] reconstructed
image with PSNR 22.97 dB

b) [16] reconstructed
image with PSNR 27.61 dB

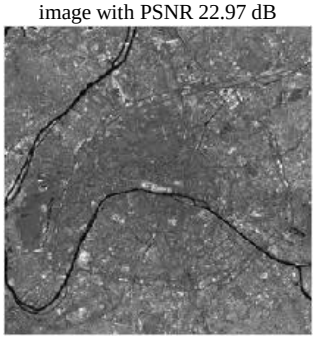

c) [9] reconstructed
image with PSNR 30.81 dB

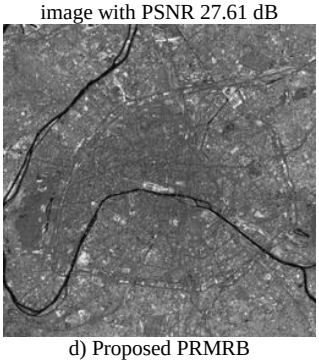

d) Proposed PRMRB
reconstructed image
with PSNR 58.38 dB

Figure 3 : Comparative Multi Spectral paris.lan
Image Reconstruction of proposed method
PRMRB with [18], [16] and [9].

For Lena.bmp image and Paris.Lan image, observations of visual comparative metric PSNR is 57.10 dB and 58.38 dB, shows an improved value compare to [18], [16] and [9], from figure 2 and figure 3. WDC.Mat and Gun.gif File images are compared with [1] and [12], the image visual results are shown in figure 4 and figure 5.

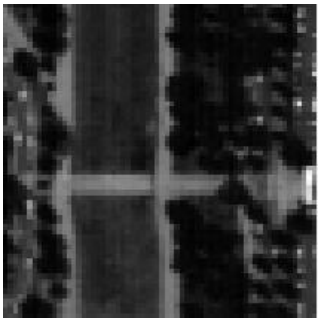

a) [1] reconstructed
image with PSNR 40.75 dB

b) [12] reconstructed
image with PSNR 31.77 dB

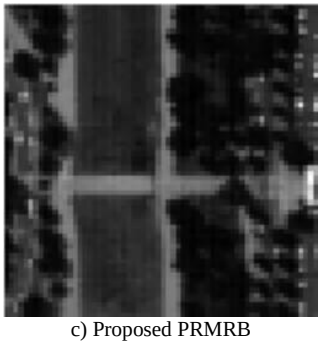

c) Proposed PRMRB
reconstructed image with PSNR 58.49 dB
Figure 4 : Comparative WDC.Mat Image
Reconstruction of proposed PRMRB
with [1] and [12].

a) [8] reconstructed
image with PSNR 35.02 dB

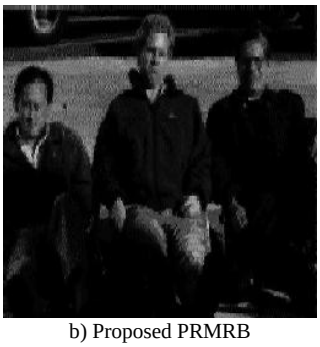

b) Proposed PRMRB
reconstructed image
with PSNR 58.21 dB

Figure 5 : Comparative Gun.gif File Image
Reconstruction of proposed PRMRB
With [8]

For WDC.mat image, observations of visual comparative metric PSNR is 58.49 dB, shows an improved value compare to [1] and [12], from figure 4. For Gun.gif image, observations of visual comparative metric PSNR is 58.21 dB, shows an improved value compare to [8], from figure 5.

B. Progressive Numerical Transmission Comparative Results:

The progressive transmission of image processing methods compared and proposed, includes image processing, coding, passing through a communication channel, decoding and image reconstruction. During these process the comparative methods [18], [16], [9], [1], [12] and [8] are considered as they are, in proposed PRMRB the test images are gone for five images. They are a) Image pre-processing stage, the data taken in different formats were pre-defined to a specific format for proposed algorithm implementation. b) Wavelet decomposition stage, to decompose the pre-processed using motion-selective rank and parallel random band selection method. c) Hybrid Discrete Multi Wavelet Transform stage, to transform the wavelet decomposed image information. d) Encoding and decoding stage, by designing a codec to transmit the decomposed image information through a contact noisy channel by adding distortions to encoded image information and decode the distorted image information for reconstruction. and e) Image performance metrics analysis stage, to compare the performance of proposed PRMRB with the literature survey methods. The performance metrics considered are :

a) *Metric:* Peak signal-to-noise ratio (PSNR)

Definition: The ratio between the maximum possible power of a signal and the power of corrupting noise that affects the fidelity of its representation.

Equation: $PSNR = 20 \cdot \log_{10}(MAX_I) - 10 \cdot \log_{10}(MSE)$.

b) Metric: Mean squared error (MSE)

Definition: The MSE represents the cumulative squared error between the compressed and the original image.

Equation: $MSE = \frac{1}{m\,n} \sum_{i=0}^{m-1} \sum_{j=0}^{n-1} [I(i,j) - K(i,j)]^2$.

c) Metric: Structural SIMilarity Index (SSIM)

Definition: The SSIM index is a full reference metric; in other words, the measurement or prediction of image quality is based on an initial uncompressed or distortion-free image as reference.

Equation: $\mathrm{SSIM}(x,y)=\frac{(2\mu_x\mu_y+c_1)(2\sigma_{xy}+c_2)}{(\mu_x^2+\mu_y^2+c_1)(\sigma_x^2+\sigma_y^2+c_2)}$.

d) Metric: Compression Ratio (CR)

Definition: CR is defined as the ratio between the uncompressed size and compressed size

Equation: $\text{Compression Ratio}=\frac{\text{Uncompressed Size}}{\text{Compressed Size}}$.

e) Metric: Bit error rate (BER)

Definition: The BER is the number of bit errors divided by the total number of transferred bits during a studied time interval.

Equation: $\mathrm{BER}=\frac{1}{2}\operatorname{erfc}(\sqrt{E_b/N_0})$.

f) Metric: Compression Time (CT)

Definition: Time taken to compress the image.

g) Metric: Reconstruction Time (RT)

Definition: Time taken to reconstruct the compressed image.

h) Metric: Feature SIMilarity Index (FSIM)

Definition: The similarity between images f1 and f2, denote by PC1 and PC2 the PC maps extracted from f1 and f2, and G1 and G2 the GM maps extracted from them. It should be noted that for color images, PC and GM features are extracted from their luminance channels. FSIM will be defined and computed based on PC1, PC2, G1 and G2.

The computation of FSIM index consists of two stages. In the first stage, the local similarity map is computed, and then in the second stage, the similarity map into a single similarity score.

Equation: $\mathrm{FSIM}=\frac{\sum_{x\in\Omega}S_L(\mathbf{x})\cdot PC_m(\mathbf{x})}{\sum_{x\in\Omega}PC_m(\mathbf{x})}$.

i) Metric: Gradient Magnitude Similarity Deviation (GMSD)

Definition: GMSD computes the local quality map by comparing the gradient magnitude maps of the reference and

distorted images, and uses standard deviation as the pooling strategy to compute the final quality score.

Equation: $GMSD=\sqrt{\frac{1}{N}\sum_{i=1}^{N}(GMS(i)-GMSM)^2}$.

j) Metric: Root Mean Square Error (RMSE)

Definition: The RMSE represents the sample standard deviation of the differences between predicted values and observed values.

Equation: $RMSError=\sqrt{1-r^2}SD_y$.

k) Metric: Image Universal Quality Index (IUQI)

Definition: IUQI is designed by modeling any image distortion as a combination of three factors: loss of correlation, luminance distortion, and contrast distortion, where local image statistics are used to define a similarity between all corresponding 8×8 blocks across input and fused images.

Equation: $Q=\frac{4\sigma_{xy}\bar{x}\,\bar{y}}{(\sigma_x^2+\sigma_y^2)\,[(\bar{x})^2+(\bar{y})^2]}$.

l) Metric: Enhancement metric (EME)

Definition: This measure averages contrast entropy over a given image using a specified block size.

Equation: $EME_{k_1,k_2}(\Phi)=\frac{1}{k_1k_2}\sum_{l=1}^{k_2}\sum_{k=1}^{k_1}\frac{I^w_{\max k,l}(\Phi)}{I^w_{\min k,l}(\Phi)}\log\frac{I^w_{\max k,l}(\Phi)}{I^w_{\min k,l}(\Phi)}$.

m) Metric: Pearson Correlation Coefficient (PCC)

Definition: The correlation coefficient r between A and B, where A and B are matrices or vectors of the same size. r is a scalar double.

Equation: $r=\frac{\sum_m\sum_n(A_{mn}-\bar{A})(B_{mn}-\bar{B})}{\sqrt{\left(\sum_m\sum_n(A_{mn}-\bar{A})^2\right)\left(\sum_m\sum_n(B_{mn}-\bar{B})^2\right)}}$.

n) Metric: Mean Absolute Error (MAE)

Definition: MAE is a measure of difference between two continuous variables. Assume X and Y are variables of paired observations that express the same phenomenon.

Equation: $\mathrm{MAE}=\frac{\sum_{i=1}^{n}|y_i-x_i|}{n}=\frac{\sum_{i=1}^{n}|e_i|}{n}$.

For the comparison of proposed PRMRB, the quality metrics were categorized in to four classes to classify the performance of comparative analysis. They are: Error Rate including M.S.E.,

B.E.R.,R.M.S.E.,E.M.E. and M.A.E., Similarity Index Results including S.S.I.M. and F.S.I.M., Compression Parameters including C.R., C.T. and C.T. and Quality Index including P.S.N.R., G.M.S.D.,I.U.Q.I. and P.C.C.

Error rate performance is tabulated in table 1. For Lena.bmp, Paris.Lan and Gun.gif images the reconstructed image has very less error rate. For WDC.Mat image the reconstructed image has medium error rate. Under the category of error rate there is a requirement of improvement R.M.S.E.

Table 1 : Numerical Comparative Results : Error Rate : [18], [16], [9], [1], [12], [8] and Proposed PRMRB

Input Image	Lena.bmp				Paris.lan				WDC.Mat			Gun.gif	
Metric	[18]	[16]	[9]	PRMRB	[18]	[16]	[9]	PRMRB	[1]	[12]	PRMRB	[8]	PRMRB
M.S.E.	155.22	15.96	9.47	3.10	327.82	112.69	53.95	0.25	0.0001	43.22	15.25	20.46	5.60
B.E.R.	0.94	0.88	0.86	0.39	0.97	0.95	0.94	0.23	1	0.52	0.65	0.78	0.61
R.M.S.E.	12.45	3.99	3.07	1.76	18.10	10.61	7.34	0.50	0.01	6.57	3.90	4.52	2.36
E.M.E.	16.98	20.98	21.80	20.56	11.73	17.44	20.44	19.86	51.48	16.85	21.37	9.80	18.11
M.A.E.	8.43	3.02	2.39	0.78	13.60	8.27	5.85	0.24	0.008	1.42	1.66	3.29	1.32

Similarity Index performance is tabulated in table 2. For Lena.bmp, Paris.Lan and Gun.gif images the reconstructed image similarity index is near to originality. For WDC.Mat image the reconstructed image similarity index need further improvement.

Table 2: Numerical Comparative Results: Similarity Index Results: [18], [16], [9], [1], [12], [8] and Proposed PRMRB

Input Image	Lena.bmp				Paris.lan				WDC.Mat			Gun.gif	
Metric	[18]	[16]	[9]	PRMRB	[18]	[16]	[9]	PRMRB	[1]	[12]	PRMRB	[8]	PRMRB
S.S.I.M.	0.97	0.99	0.99	0.99	0.98	0.99	0.99	0.99	0.98	0.99	0.99	0.51	0.83
F.S.I.M.	0.87	0.97	0.98	0.99	0.73	0.93	0.96	0.99	0.99	0.98	0.98	0.92	0.99

Compression Parameters performance is tabulated in table 3. For Lena.bmp, Paris.Lan, WDC.Mat and Gun.gif images the reconstructed image has C.R.=1. Under the category of C.T. and R.T., these values are more comparatively to make the proposed PRMRB improvements in visual quality metrics.

Table 3: Numerical Comparative Results: Compression Parameters: [18], [16], [9], [1], [12], [8] and Proposed PRMRB

Input Image	Lena.bmp				Paris.lan				WDC.Mat			Gun.gif	
Metric	[18]	[16]	[9]	PRMRB	[18]	[16]	[9]	PRMRB	[1]	[12]	PRMRB	[8]	PRMRB
C.R.	1	1	1	1	1	1	1	1	1	1	1	1	1
C.T.	3.91	2.57	4.74	28.08	3.86	3.07	5.81	31.52	0.02	15.60	28.67	1.11	29.94
R.T.	3.76	1.27	2.22	27.71	3.75	1.68	3.14	29.41	11.40	0.003	27.31	1.58	28.31

Quality Index performance is tabulated in table 4. For Lena.bmp, Paris.Lan and Gun.gif images the reconstructed image has very high P.S.N.R. and I.U.Q.I. value. P.C.C. and G.M.S.D. values are very near to ideal values.

Table 4 : Numerical Comparative Results : Quality Index : [18], [16], [9], [1], [12], [8] and Proposed PRMRB

Input Image	Lena.bmp				Paris.lan				WDC.Mat			Gun.gif	
Metric	[18]	[16]	[9]	PRMRB	[18]	[16]	[9]	PRMRB	[1]	[12]	PRMRB	[8]	PRMRB
P.S.N.R.	26.22	36.09	38.36	57.10	22.97	27.61	30.81	58.38	40.75	31.77	58.49	35.02	58.21
G.M.S.D.	0.10	0.01	0.008	0.001	0.15	0.04	0.02	0.008	0.003	0.03	0.009	0.03	0.003
I.U.Q.I.	0.61	0.86	0.89	0.98	0.35	0.77	0.89	0.99	0.97	0.97	0.96	0.34	0.83
P.C.C.	63683	65358	65434	65500	48391	60263	63081	65523.8	40840	64198	65252.2	40252	65410.6

From the table 4, the quality index parameters are very near to ideal values. Proposed method concentrates in improving the visual performance by keeping the time parameters and error rate at lower level of improvement.

IV. Conclusions

Band selection of MR image made subband coefficients with low bit rate and high quality bits making the accurate wavelet decomposition and reconstruction. Band selection region $i_{Mr}(x, y)$ is varied in the ranges of 4,8,16,32,64,128 and 256, this range improves the similarity index of reconstructed image comparatively. Random selective process is varied according to the band level and motion variation, making the continuous and discrete subband nodes to be selective and regenerative for the development of new multiwavelet principles. PRMRB de-correlative stretch results into a multidirectional band to provide access to random filter design. These random filters improved the visual quality of reconstructed image comparatively by varying the

$i_{multi-d(\upsilon_x+\upsilon_y)}(x,y)$ in design. By selecting the $i_{Me(\upsilon_x+\upsilon_y)}(x,y)$ =1, further image error rate is minimized. Band selected image is mapped through $i_{map(\upsilon_x+\upsilon_y)}(x,y)$, by selecting the mapping structure as map:band as 4:1, 16:4, 32:1 and 64:4, this range improves the time parameters of reconstructed image comparatively. The comparative results clearly shows the improvement of S.S.I.M and P.S.N.R. values for any type of image format. By observing the visual reconstructed images and numerical performance metrics of proposed PRMRB with different image processing methods, comparatively have shown a better MR image compression.

V. Future Work

PRMRB is implemented through motion based hybrid multidirectional multiwavelet decomposition with visual accurate reconstruction from a sensitive MR image to complex MS image, showing a new direction in the field of video processing. PRMRB band classification and direction analysis makes multi-subband selection possible, making a new approach to detail subband selection process. PRMRB implementation motivates high quality video compression method through wired distorted channel, for high visual quality results and very less error rates.

References;

[1]. K. Ma et al., "Robust Multi-Exposure Image Fusion: A Structural Patch Decomposition Approach , "IEEE Trans. on Image Processing, vol. 26, issue 5, pp. 2519 - 2532, 2017.

[2]. S. Jagadeesh and E. Nagabhooshanam, "Energy Interpolated Mapping for Image Compression with Hierarchical Coding, " Indian Journal of Science and Technology, vol 10 (9), pp- 1-10, 2017.

[3]. Miguel A. Veganzones et al., " Hyperspectral Super-Resolution of Locally Low Rank Images From Complementary Multisource Data, " IEEE Trans. on Image Processing, vol. 25, no. 1, pp-274-288, 2016.

[4]. S.Jagadeesh, E.Nagabhooshanam, "Scalable Identity Wavelet in Hierarchical Image Codec", IOSR Journal of VLSI and Signal Processing(IOSR-JVSP), Volume 6,Issue 6, Ver.1 (Nov-Dec. 2016), pp 01-12.

[5]. S. Jagadeesh and E. Nagabhooshanam, " Multi Spectral Band Selective Coding for Medical Image Compression, " Global Journal of Computer Science and Technology: F, Graphics & Vision, vol. 15, issue 3, pp-21-28 2015.

[6]. Jagadeesh, S.E. Nagabhooshanam. "Linear adaptive global node-tree filters based SPIHT MR image codec," in Proc. of IEEE Conf. on Electrical, Computer and Communication Technologies, pp.1-8, March 5-7, 2015.

[7]. S.Jagadeesh, Dr. E. Nagabhooshanam, "Embedded Zero Binary Tree Wavelet Based SPIHT" in National Conference on Communications, Signal Processing & Systems (NCCSPS - 2014) during 24- 25, August 2014, conducted by Department of ECE, JNTUH College of Engineering, Hyderabad.

[8]. B. K. Shreyamsha Kumar, "Multifocus and Multispectral Image Fusion based on Pixel Significance using Discrete Cosine Harmonic Wavelet Transform", Signal, Image and Video Processing, vol. 7, issue 6, pp. 1125-1143, 2013.

[9]. K. K. Huang and D. Q. Dai, "A new on-board image codec based on binary tree with adaptive scanning order in scan-based mode," IEEE Transactions on Geoscience and Remote Sensing, vol. 50, no. 10, pp. 3737-3750, 2012.

[10]. Yuming Fang et al., "Bottom-Up Saliency Detection Model Based on Human Visual Sensitivity and Amplitude Spectrum, "IEEE Trans. on Multimedia, vol. 14, no. 1, pp-187-198, 2012.

[11]. José M. Bioucas-Dias et al., " Hyperspectral Unmixing Overview: Geometrical, Statistical, and Sparse Regression-Based Approaches, " IEEE Journal of Selected Topics In Applied Earth Observations And Remote Sensing, vol. 5, no. 2, pp-354-379, 2012.

[12]. Lidan Miao et al., "Binary tree-based generic demosaicking algorithm for multispectral filter arrays, "IEEE Trans. on Image Processing, vol 15 no. 11, pp-3550-3558, 2006.

[13]. Ivan W. Selesnick, " The Double-Density Dual-Tree DWT, " IEEE Trans. on Signal Processing, vol 52 no. 5, pp-1304-1314, 2004.

[14]. Zhou Wang et al., "Image Quality Assessment: From Error Visibility to Structural Similarity, " IEEE Trans. on Image Processing, vol 13 no. 4, pp-1-14, 2004.

[15]. Ivan W. Selesnick, " Interpolating Multiwavelet Bases and the Sampling Theorem, " IEEE Trans. on Signal Processing, vol 47 no. 6, pp-1615-1621, 1999.

[16]. Amir Said and William A. Pearlman, "A New Fast and Efficient Image Codec Based on Set Partitioning in Hierarchical Trees," IEEE Transactions on Circuits and Systems for Video Technology, vol. 6, pp. 243-250, 1996.

[17]. Xiang-Gen Xia et al., " Design of Prefilters for Discrete Multiwavelet Transforms, " IEEE Trans. on Signal Processing, vol 44 no. 1, pp-25-35, 1996.

[18]. J. M. Shapiro, "Embedded image coding using zerotrees of wavelet coefficients," IEEE Transactions on Signal Processing, vol. 41, no. 12, pp. 3445-3462, 1993.

IOSR Journal of Computer Engineering (IOSR-JCE) is UGC approved Journal with Sl. No. 5019, Journal no. 49102.

B. Sridhar Parallel Random Motion-Selective Rank Band Based Image Compression Using Hybrid Multi Wavelet Transform." IOSR Journal of Computer Engineering (IOSR-JCE) , vol. 19, no. 5, 2017, pp. 23-34.